Alkali activated solidification/stabilisation of air pollution control residues and co-fired pulverised fuel ash

Robin Shirley, Leon Black*

School of Civil Engineering, University of Leeds, Leeds LS2 9JT, UK

ABSTRACT

This paper examines the potential treatment by solidification/stabilisation (S/S) of air pollution control (APC) residues using only waste materials otherwise bound for disposal, namely a pulverised fuel ash (PFA) from a co-fired power station and a waste caustic solution. The use of waste materials to stabilise hazardous wastes in order to meet waste acceptance criteria (WAC) would offer an economical and efficient method for reducing the environmental impact of the hazardous waste. The potential is examined against leach limits for chlorides, sulphates and total dissolved solids, and compressive strength performance described in the WAC for stable non-reactive (SNR) hazardous waste landfill cells in England and Wales. The work demonstrates some potential for the treatment, including suitable compressive strengths to meet regulatory limits. Monolithic leach results showed good encapsulation compared to previous work using a more traditional cement binder. However, consistent with previous work, SNR WAC for chlorides was not met, suggesting the need for a washing stage. The potential problems of using a non-EN450 PFA for S/S applications were also highlighted, as well as experimental results which demonstrate the effect of ionic interactions on the mobility of phases during regulatory leach testing.

© 2011 Elsevier B.V. All rights reserved.

1. Introduction

Air pollution control (APC) residues collected when controlling the composition of flue gas emissions during the incineration of solid waste in modern energy from waste (EfW) facilities, have an absolute hazardous entry in the European Waste Catalogue [1]. Untreated residues frequently exceed UK regulatory leach limits, even for hazardous waste landfill sites [2]. This is commonly due to the leaching of chlorides and heavy metals such as lead (Pb) and zinc (Zn), although the variability in the composition of the residues means that waste acceptance criteria (WAC) limits may be surpassed by a number of pollutants [3].

Close to 200,000 tonnes of APC residues are produced per annum in the UK [4], a figure rising with increasing use of EfW incineration as a waste management option, in line with government strategy [5–7]. These residues are often stored in deep salt mines or partially stabilised and sent to specific landfill sites with a 3-times derogated WAC. Derogated criteria are designed to allow flexibility when dealing with particular problem wastes and are subject to an annual review of alternative options for managing the waste [8], but the current approach is not considered a long term option and

sustainable technologies for the treatment of APC residues require development.

Many potential treatment methods for APC residues have been proposed [9–11]. Amongst these treatment options is solidification/stabilisation (S/S); the process of mixing the waste with supplementary materials in order to form a solid monolith in which waste elements may be immobilised chemically and physically by the reaction products. There is a considerable body of work on the S/S of APC residues or incinerator fly ash, including use of cement, blast furnace slag, coal fly ash or blends of these materials [12–19]. The potential for S/S with these materials hinges on the possibility of binding components through methods including surface sorption, chemical incorporation and physical encapsulation via the formation of minerals such as ettringite, Friedel's salt, calcium silicate hydrates and calcium aluminosilicate hydrates [15,20–23]

Previous work has highlighted the considerable difficulty in immobilising the very high amounts of chlorides present in APC residues due to the paucity of insoluble chloride-bearing reaction products, with much of the chloride reported to be present as soluble salts, e.g. NaCl, KCl and CaClOH [19]. Though Friedel's salt, a phase known to form when APC residues are mixed with calcium aluminate cements [15], Portland cement [17,19], GGBS [19] and pozzolanic cement [18], may offer some potential for immobilisation of chloride [15,24], leach test results suggest this phase has little chloride-binding potential when immobilising APC residues with Portland cement [13,17]. This may be due to inherently low

* Corresponding author. Tel.: +44 113 343 2283; fax: +44 113 343 2265.
E-mail addresses: cnrs@leeds.ac.uk (R. Shirley), l.black@leeds.ac.uk (L. Black).

quantities of Friedel's salt being formed, or the APC residues raising the pH of the pore water, reducing Friedel's salt's stability [24]. The potential for metal binding in these reaction products has however been shown [12,16–18].

This study has used PFA from a co-fired (coal and biomass) power station and a concentrated waste caustic solution. The PFA is deemed unsuitable for construction purposes according to EN450 [25] and is therefore subject to disposal. With increasing use of co-firing in UK power stations to gain Renewable Obligation Certificates, such PFAs may become more commonplace and therefore finding uses for them is desirable.

PFA offers the opportunity for S/S due to its high Si and Al content, enabling cementation through pozzolanic reactions with the Ca from the APC residues. Poon et al. [26–28] demonstrated the pozzolanic potential of a similarly high carbon rejected fly ash in high calcium S/S systems using synthetic heavy metal sludge. The use of traditional or co-fired PFA for immobilisation of APC residues has however not to the authors' knowledge been reported without cement addition.

The other waste material used in this study was an aluminium-containing NaOH solution from an industrial cleaning process. The potential use of alkali activated cement as a waste binder has been discussed extensively in the literature, and is summarised well in [29,30]. There are indications that alkali activated cements result in a less porous, more durable matrix which is beneficial for waste encapsulation [29–31]. Various forms of C–S–H have been identified as primary reaction product in alkali activated pozzolanic blends [32–35], but alkali activation of PFA can also allow precipitation of zeolitic species, with potential cation exchange capacities as high as 5 mEq/g [36], and may exist alongside C–S–H [35,37]. Alkali activation may also increase the rate of reaction in pozzolanic systems [27,33,35,38,39], due to the greater rate of chemical dissolution. This acceleration may enable commercially feasible setting times and strength development by accelerating otherwise slow reactions, but reaction products, microstructure and ultimately performance are also heavily dependent on the raw material composition and the curing conditions [31,40].

The use of a NaOH solution to activate a pozzolanic S/S matrix containing APC residue has not previously been reported, though the use of a strong alkali solution to produce a geopolymeric binder for APC residues or incinerator fly ash has been reported [41–44]. The residue used by Kourti et al. [41] had been plasma treated with quartz and corundum so there was no risk of failing WAC, therefore solidification was the goal and stabilisation was not a concern, whilst the other studies showed the potential to reduce mobility of several metals but chlorides remained present as highly mobile phases [42,43].

The performance of this treatment was assessed based on the WAC for stable non-reactive (SNR) hazardous waste and non-hazardous waste deposited in the same cell with such waste [2], and the criteria described by Stegemann and Zhou [45] for S/S treatments. Criteria examined include workability, setting time, UCS, and leach performance in granular and monolithic tests. Several mixes have been examined in order to assess the effects of varying key properties including; l/s, APC residue:PFA ratios and curing duration and temperature. Characterisation was also undertaken so as to understand the science underpinning the performance.

2. Experimental

2.1. Materials

The APC residue studied in this work arose from the incineration of solid waste in a UK Energy from Waste incinerator. The composition is similar to those discussed in several papers [3,4,46–49].

Table 1
Elemental composition of materials (%w/w), WC = waste caustic solution.

Element	Ca	Cl	Si	Al	Na	K	Pb	Zn	S	LOI
APC	46	20	0.24	0.08	1.4	0.5	0.17	0.19	0.65	5.4
PFA	3.07	0.04	24.06	10.22	0.83	1.94	0.00	0.21	3.75	10.4
WC					2.65	7.96				

The co-fired PFA came from a UK coal power station burning coal and biomass with a minimum of 80% coal by dry mass (EN 450). The aluminium-containing waste caustic solution (WC) was from an industrial cleaning process, similar to that discussed by Tansens et al. [50].

Table 1 shows the chemical compositions of the PFA and WC determined by XRF and the composition of the APC residue determined by total acid digestion and ICP-OES/MS. The WC composition was determined by evaporating the solution to dryness, determining the dry weight and then performing XRF analysis. Values given in Table 1 are as a %w/w of solution i.e. TDS was 10.61% (106,100 mg/kg). This sodium content equates to a 3.5 M NaOH solution.

2.2. Solidified product preparation

Samples were prepared as 50 mm cubes by mixing until homogenous and compacted using a vibrating table or hand tamping as necessary. Samples were cured at various constant temperatures and ambient humidity until test age. Table 2 shows the composition of all the mixes along with the shorthand identification used. These mix designs were selected based on preliminary test results for workability and compressive strength which showed an apparent optimum close to a composition 40% APC residue, 60% PFA and a l/s ratio of 1, i.e. sample 2:3 l/s = 1. The default curing temperature was 38 °C, but other samples were cured at room temperature (23 °C) or 80 °C. Following work by Stegemann and Zhou [45], some samples were cured for 21 days and submerged in water at room temperature for 7 days before testing.

2.3. Mix and block characterisation

2.3.1. Physical tests
Relevant standards were used to characterise blocks with respect to workability [51], setting time [52] and compressive strength [53] with the latter test adapted to use 50 mm cubes.

2.3.2. Leach testing
Granular leach tests were performed on blocks cured for 28 days according to the batch extraction test with l/s = 10, BS EN 12457-2:2002 [54]. The method was adapted to accommodate the use of a rotating table operating at 90 rpm rather than an end-over-end tumbler. A brief test showed only slight differences in the chloride leach from anhydrous APC residue with stirring opposed to tumbling, with the former giving a mean release of 166,033 mg/kg with σ = 26,565 mg/kg and tumbling releasing 160,000 mg/kg. Thus, whilst it is appreciated that results from a rotating table will not be identical to those obtained with an end over end tumbler, the

Table 2
Mix compositions per 100 g and shorthand nomenclature used.

Mix nomenclature	APC (g)	PFA (g)	WC (g)	l/s	Curing temp (°C)
1:4 l/s = 0.55	12.9	51.6	35.5	0.55	38
1:4 l/s = 0.75	11.4	45.6	43	0.75	38
1:4	10	40	50	1	38
2:3	20	30	50	1	23/38/80
3:2	30	20	50	1	38

chloride release is similar, and the test still enables the performance of the mixes to be compared with one another.

Anion leach was examined using a Dionex chromatograph with ion exchange separator column. The pH of the leachate was also measured along with total dissolved solids (TDS) by monitoring dry weights.
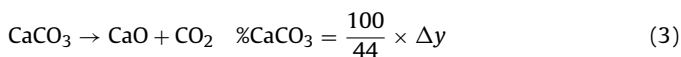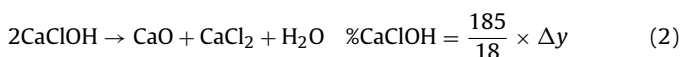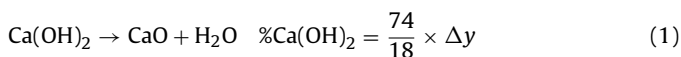
Monolithic leach tests were conducted on 50 mm cubes after 28 days' curing according to the static test, EA NEN 7375 [55]. Tests were conducted with a water volume 5-times the volume of the test piece.

2.3.3. Acid neutralisation capacity (ANC)

ANC was performed according to DD CEN/TS 15364:2006 [56] although intervals of greater than 1.5 pH units were allowed between consecutive pH values. pH was measured with additions of 1, 2, 3, 4 and 10 mEq/g to give a comparison of ANC between samples.

2.3.4. Characterisation techniques

Simultaneous thermal analysis (STA), i.e. simultaneous thermogravimetric (TG) and differential thermal analysis (DTA), was performed on a Stanton Redcroft STA 1500. Tests were run under a nitrogen atmosphere with a heating rate of 20 °C/min from 20 to 1000 °C. Peaks were quantified using the weight loss indicated by the TG curve and Eqs. (1)–(3). This weight loss was determined using tangents to account for the sloping baseline due to gradual water loss.

$$Ca(OH)_2 \rightarrow CaO + H_2O \quad \%Ca(OH)_2 = \frac{74}{18} \times \Delta y \tag{1}$$

$$2CaClOH \rightarrow CaO + CaCl_2 + H_2O \quad \%CaClOH = \frac{185}{18} \times \Delta y \tag{2}$$

$$CaCO_3 \rightarrow CaO + CO_2 \quad \%CaCO_3 = \frac{100}{44} \times \Delta y \tag{3}$$

In which Δy is the % weight loss due to loss of H_2O or CO_2, as appropriate. Overlapping mass losses due to portlandite and CaClOH were distinguished by differentiating the TG curve and performing peak fitting to determine relative areas. These relative areas were then applied to the percentage weight loss over the temperature range of 350–600 °C to determine the losses attributable to the decomposition of either peak.

Monitoring the density of the mixes when fresh and at each test age allowed normalisation of STA quantification. Results were normalised as a %w/w of the fresh mix using Eq. (4).

$$\%W_f = \left(\frac{D_t}{D_f}\right) \times \%W_t \tag{4}$$

In which $\%W_f$ is the weight percentage of a compound in the fresh mix calculated by analysis of anhydrous materials and dilution; $\%W_t$ is the weight percentage of a compound at the test age; D_t is the density of the mix at the test age; D_f is the density of the fresh mix

This approach was used to monitor the calcium hydroxide content over time, which gave an indication of any pozzolanic reaction. Also, Eq. (4) was rearranged and D_t replaced with dry mass density at test age t, determined by drying at 105 °C for 24 h, to calculate the availability of elements in mg/kg$_{dry\ mass}$. This allowed interpretation of leach results.

Sample morphology and composition was also examined by low-vacuum scanning electron microscopy, using a Phillips XL-30 environmental SEM fitted with gaseous secondary electron (GSE) and backscattered electron (BSE) detectors, plus energy dispersive X-ray (EDX) analysis. Anhydrous materials were viewed as-received, by dusting a small quantity of material onto a carbon pad.
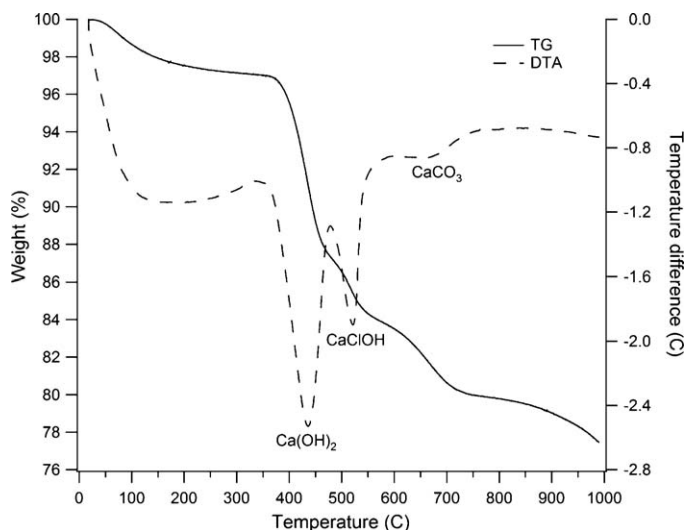

Fig. 1. STA analysis of as received APC residue.

X-ray diffraction (XRD) was performed using a Phillips X'pert Pro diffractometer with X'celerator detector; Cu Kα X-ray source operated at 40 kV and 40 mA; Ni β filter; 0.04 radian Soller slits; divergence and anti-scatter slits programmed to give an irradiated/observed length of 10 mm and a spinner revolution time of 4 s per revolution.

3. Results and discussion

3.1. Anhydrous APC residue characterisation

In addition to the elemental composition determined by ICP OES/MS, the anhydrous APC residue was characterised by XRD and STA. STA (Fig. 1) revealed the presence of $Ca(OH)_2$, CaClOH and $CaCO_3$. XRD meanwhile showed the presence of these phases plus NaCl (Fig. 2), with semi-quantitative XRD analysis showing similar levels of NaCl and $CaCO_3$. These phases have all previously been observed in APC residues [46,49,57–59]. Quantification of the calcium-bearing phases by STA is shown in Table 3. Portlandite was the predominant phase, arising from the use of a lime scrubber. CaClOH formed from the reaction of lime or hydrated lime with the acid gas HCl, as shown in Eqs. (5) and (6) [60,61]. Calcite formed from carbonation of the lime.

$$CaO + HCl \rightarrow CaClOH \tag{5}$$

$$Ca(OH)_2 + HCl \rightarrow CaClOH + H_2O \tag{6}$$
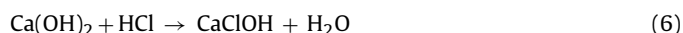
SEM analysis of the APC residue showed agglomerated fine particles [12,13,15,49], with impact on the practical particle size distribution and active surface area. Fig. 3 shows a BSE micrograph revealing the presence of small, isolated 'specks' of Pb, Zn and Cu, (identified by EDX analysis). The feature in the top left hand corner of Fig. 3 was identified as a carbon deposit.

Table 3
%w/w composition of residue as received, after leach testing according to BS EN 12457-2, and after mixing with NaOH, determined by STA.

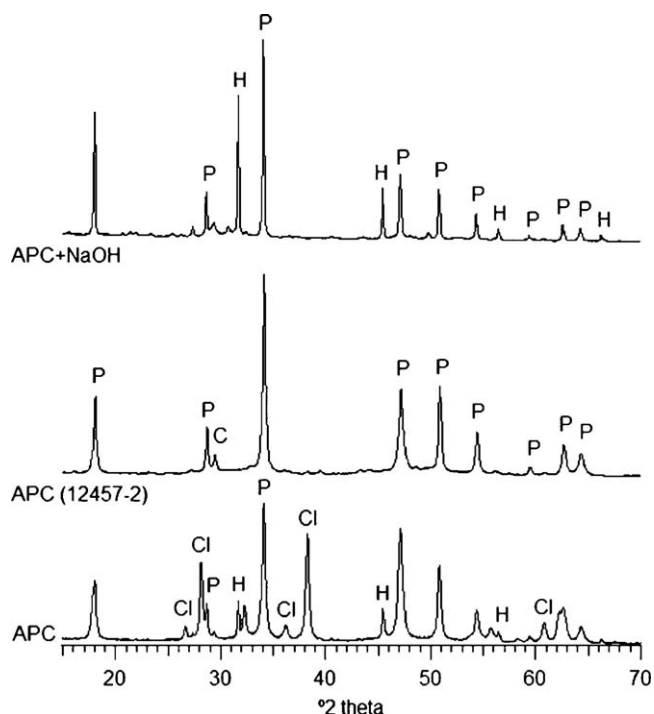| Compound	APC residue (as received)	APC residue after 12457-2[a]	APC residue + NaOH
$Ca(OH)_2$	37.8	63.3	50.9
CaClOH	16	0	0
$CaCO_3$	4.3	16.3	10.6

[a] % as analysed, not corrected for TDS.

Fig. 2. XRD plot of APC residue as received, following leaching according to BS EN 12457-2, and following mixing with NaOH. P = Ca(OH)$_2$, Cl = CaClOH, H = NaCl, C = CaCO$_3$.

A significant fraction of the APC residue was solubilised during BS EN 12457-2 (TDS = 280,000 mg/kg). Chloride release of 160,000 mg/kg during the same test indicated the majority of this soluble fraction to comprise the CaClOH and NaCl, confirmed by XRD and STA analysis (Fig. 2 and Table 3).

3.2. Anhydrous co-fired PFA characterisation

A typical hump was visible in the XRD analysis of the PFA with a maximum ~23–27° 2θ indicating a siliceous glass structure [62]. This large glass content is beneficial for the pozzolanic activity of the ash [35,63]. There was also crystalline Si and Al present as quartz and mullite. XRD revealed trace levels of potassium sulphate as the only crystalline sulphur-bearing phase. This suggests that the sulphur present in the anhydrous PFA is in amorphous forms, potentially as organic sulphur. Reduced and intermediate forms of sulphur may be present rather than oxidised sulphur (sulphate)
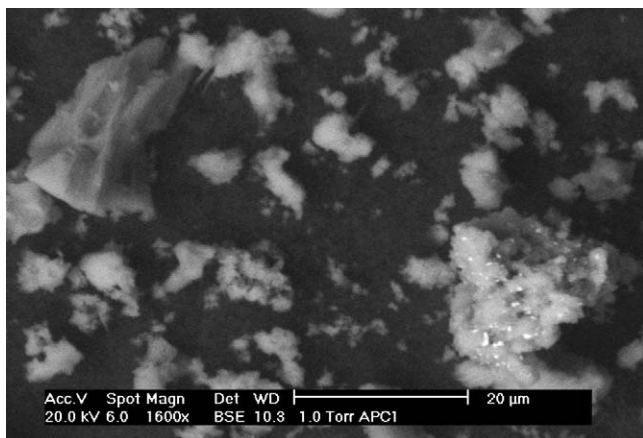

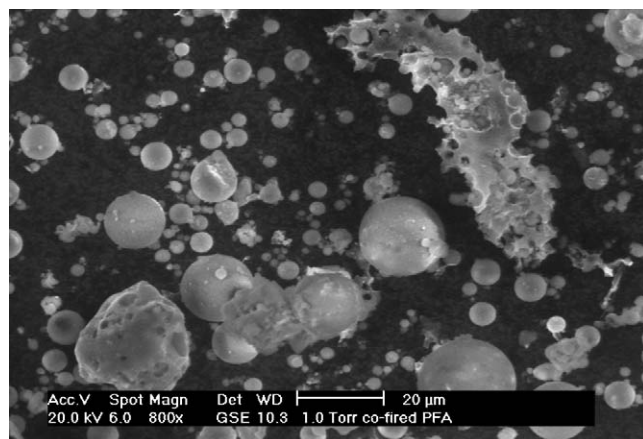**Fig. 3.** BSE SEM image of APC residue as received.

Fig. 4. GSE SEM image of co-fired PFA as received.

when combustion is incomplete or there are non-equilibrium conditions within the combustion system [64]. The presence of high levels of unburnt carbon is also indicative of incomplete combustion.

A high sulphur content can be problematic in conventional Portland cement:PFA blends since it upsets the sulphur to aluminium balance, which can impact on concrete durability and soundness. Because sulphate release must be monitored in order to comply with WAC, high sulphur content in an S/S matrix can also be problematic. The sulphur content in this ash exceeds the SO$_3$ upper limit of 3% stipulated by EN 450, and sulphate release from the untreated PFA was 2800 mg/kg during BS EN 12457-2. Both EN 450, and BS 8500, limits are also exceeded by the 10.4% loss on ignition (LOI) of the PFA, which is primarily a result of unburnt carbon. Vesicular carbon particles were observed by GSE imaging (Fig. 4) and occasionally revealed trace molybdenum deposits by EDX analysis. Spherical particles, typical of conventional PFA, with a large size distribution were also seen. 45 μm sieve retention was 33.7%; which is much coarser than many of those reported previously [65]. Coarse PFAs tend to suffer a reduced rate of reaction and increased water demand for a given workability [65]. Water demand is also particularly increased when there is a high carbon content [65,66].

3.3. Physical tests

Table 4 shows the key engineering properties of the various mixes. As found previously [13,14] mix workability decreased with l/s or as APC residue content was increased. The latter observation is due to the hygroscopic nature of the residues owing to a high deliquescent salt content [13] and the fineness of the residue compared to that of the PFA. There was a significant density difference between water and the waste caustic solution (1.216 kg/L) which affected the volume of liquid used when working on a w/w basis. Equivalent mixes were considerably more workable when mixed

Table 4
Physical performance of S/S products.

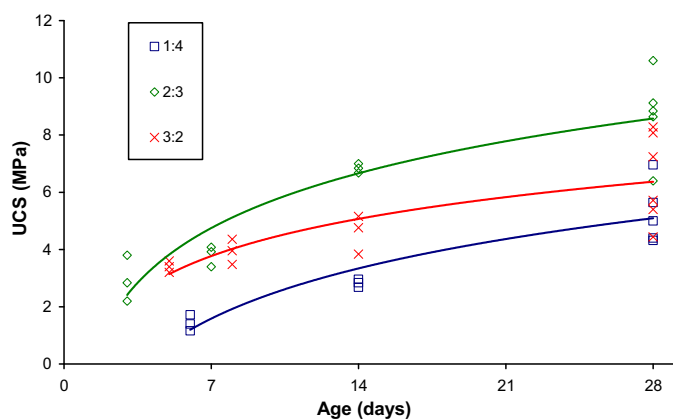| Mix	Flow value (mm)	Final setting time (h)	28d UCS (MPa)	%UCS loss (7d sub)
1:4 (0.55)	145	14.75	13.4	8
1:4 (0.75)	215	22	10.1	19
1:4	>Testable	31.75	4.6	56
2:3 (23)	180	120.75	3.0	−80
2:3	180	31.25	8.7	14
2:3 (80)	180	5.75	7.9	47
3:2	135	49	6.5	4

Fig. 5. Effect of varying APC residue:PFA ratio on UCS of mixes at l/s = 1, cured at 38 °C.

with water. Stegemann and Zhou [45] suggest a target flow value for S/S applications of > ~175 mm to facilitate casting. To meet this criterion with APC residue contents >40%w/w$_{dry}$ (2:3), a l/s > 1 would be required, but as will be seen later, increasing l/s had serious implications for structure and durability.

Setting times increased with increasing APC residue content, as reported previously, possibly due to the increased heavy metal content which is known to retard hydration [13,14,67–69]. This increase appeared to be offset by the increased consistency of sample 1:4 compared to sample 2:3.

Table 7 also shows 28 day compressive strength and the percentage loss in strength when the samples were immersed in water for the final 7 days of curing. The effects of the different parameters on the first 28 days' strength development can be seen in Figs. 5–7.

Fig. 5 shows the effect of varying the APC residue:PFA ratio on compressive strength development of mixes with l/s = 1. Mixes 1:4, 2:3 and 3:2 therefore had %w/w$_{dry}$ APC residue contents of 20, 40 and 60% respectively (Table 2). Since strength development is due overwhelmingly to pozzolanic reactions, then the variation in Ca/Al + Si as the APC residue:PFA ratio was changed can be assumed to have significant impact on the UCS [70] (see compositions in Table 1). The variations in plastic behaviour of the mixes, and therefore the degree of compaction achieved also played a considerable role in strength development. Although the compaction factor was not measured, greater compaction of dry mass when mixing with higher APC residue contents was evident. This contributed to higher strengths, reduced porosity and permeability as discussed later. Fig. 6 meanwhile shows that, as would be expected, increased l/s
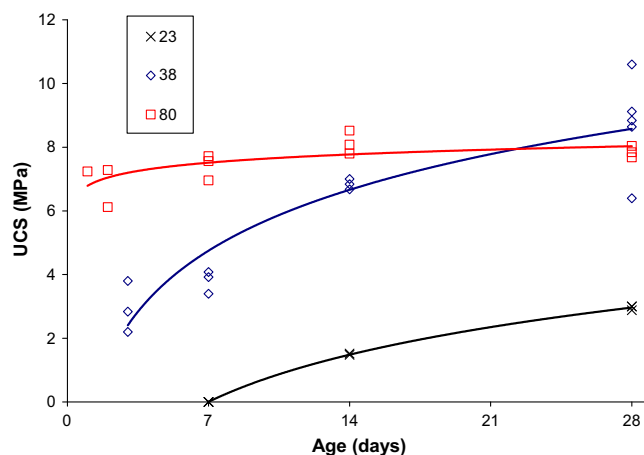

Fig. 6. Effect of l/s variation on UCS, at APC residue:PFA = 1:4, cured at 38 °C.

Fig. 7. Effect of curing temperature on UCS at APC residue:PFA = 2:3 and l/s = 1. *Note*: Samples cured at room temperature (23 °C) did not suffer acceptable failure according to BS EN 12390-3:2009 at 7 days and were not testable prior to this.

ratios resulted in reduced strength [71], primarily due to increased porosity.

Use of excess heat at an on site treatment facility would provide an economical method of increasing curing temperature should it be beneficial. Fig. 7 shows the significant effect of curing temperature on the strength development of mix 2:3, over 28 days. At 23 °C strength gain was both slight and slow, with samples remaining malleable and therefore not suffering acceptable failure according to BS EN 12390-3:2009 at 7 days. With an increase in curing temperature to 38 °C there was more pronounced strength development, including at early age (3 days). This pattern is consistent with strength development of pozzolanic systems at various curing temperatures where moderately elevated temperatures are required to induce strength development [72]. As the curing temperature was raised to 80 °C, early-age strength was much greater. At 80 °C 80–90% of the maximum strength was developed during the first 24 h, and the maximum UCS appeared to be achieved after 14 days. After 28 days the strength was less than that of the mix cured at 38 °C. Such behaviour is not unknown in cement science, where high curing temperatures induce more rapid hydration, and therefore higher early age strength, but result in uneven distribution of hydration products and possible resistance to complete hydration. Such conditions result in a more open microstructure and therefore lower later-age strength [33,73–75]. The age at which temperature is detrimental to UCS occurred much later here than reported by Puertas et al. [32] or Wang et al. [33] when studying NaOH activated blends of PFA/GGBS or PFA/CKD respectively; perhaps due to a lower initial reactivity of the materials used here.

All of the samples surpassed the 1 MPa strength threshold (before and after submersion) for SNR WAC. However, most samples showed a considerable loss of strength after submersion, due to the washing out of significant quantities of solids. However, there were a number of factors influencing the extent of strength loss. Increased l/s or curing temperature resulted in a greater loss in strength after submersion in water for 7 days due to the more porous, permeable microstructure. Samples cured at room temperature showed an increase in strength after submersion, despite considerable TDS. This suggests production of minerals with significant contribution to UCS between 21 and 28 days, such as C–S–H, overwhelmed the strength loss due to TDS. Finally, APC residue content also had an effect, with the percentage loss in strength decreasing as the APC residue content increased. This was despite the increased soluble fraction with increasing APC residue content, and indicated a less permeable matrix at higher APC residue contents, most likely due to the greater degree of compaction.
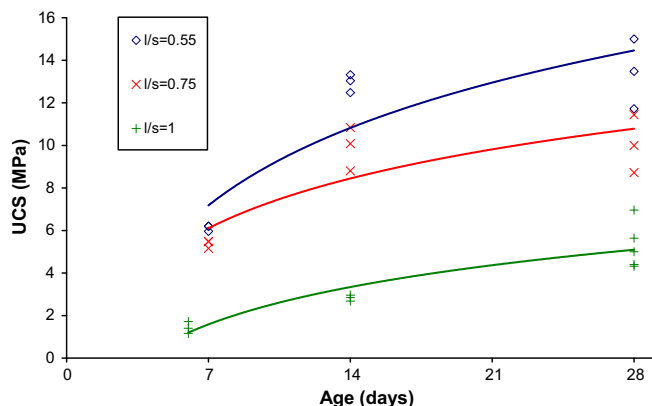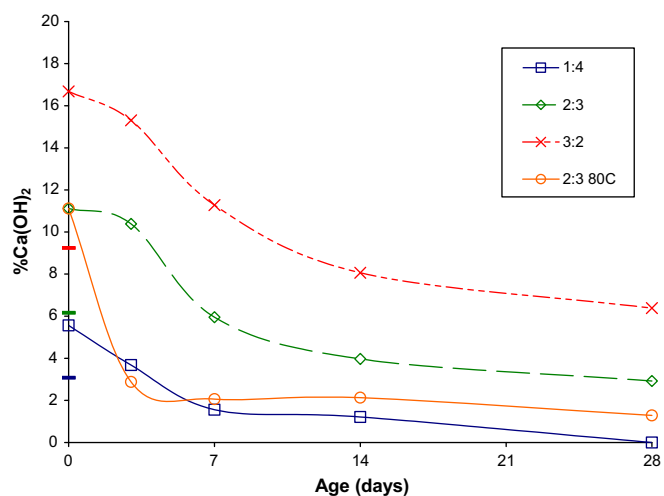
Fig. 8. Ca(OH)$_2$ content of samples over 28 days (%w/w), determined by STA. Dashes on the y axis indicate starting contents of Ca(OH)$_2$ without allowing for Eq. (7) (3:2 > 2:3 > 1:4). Initial values are calculated based on empirically determined data in Table 3 and dilution.

3.4. Characterisation of products

The degree of pozzolanic activity was measured by monitoring changes in Ca(OH)$_2$ and CaCO$_3$ content over time by STA (Fig. 8). All samples no longer exhibited the mass loss at a little above 500 °C attributed to CaClOH. This was due to this phase's conversion to Ca(OH)$_2$ when mixed with NaOH, as shown in Eq. (7).

$$CaClOH + NaOH \rightarrow NaCl + Ca(OH)_2 \qquad (7)$$
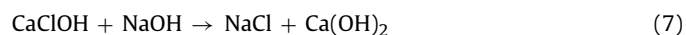
This was confirmed by mixing a quantity of APC residue with a laboratory NaOH solution before drying in a vacuum desiccator and analysing by XRD and STA (Table 3 and Fig. 2). This interaction between CaClOH and NaOH has also been suggested by Zheng et al. [43] based on XRD observations.

A consequence of this reaction was an increase in Ca(OH)$_2$ content, in all samples, compared to that calculated based upon analysis of the anhydrous materials and dilution (marked as dashes intersecting the y axis in Fig. 8). The empirically determined composition of the APC residue after mixing with NaOH (Table 3) was used to calculate the initial Ca(OH)$_2$ content in the mixes as displayed in Fig. 8.

In all cases the Ca(OH)$_2$ contents diminished over time, confirming a pozzolanic reaction concurrent with strength development. Comparing the results from the 2:3 mixes cured at 38 and 80 °C, consumption of Ca(OH)$_2$ was more rapid at higher temperature, corresponding to the much greater rate of strength gain as reported earlier. However, other factors also influence strength, such as microstructure, since the mix cured at higher temperatures ultimately showed a lower Ca(OH)$_2$ content; indicative of a more extensive reaction, despite the lower 28 day strength. Fig. 8 also shows how the Ca(OH)$_2$ content at all ages increased with increasing APC residue content. Sample 3:2 showed a considerable excess of Ca(OH)$_2$, with a detrimental effect on strength.

Excess Ca(OH)$_2$ could have several implications for the long term performance of the S/S product. Over time it could carbonate, causing a drop in pH and buffering capacity, with significant implications on the leach behaviour [47,63,76–78]. Carbonation is an expansive reaction and so may reduce the porosity of the matrix, increasing the extent of physical encapsulation of the waste as suggested in [79]. However, excessive expansion could result in cracking, reducing durability and encapsulation [76]. Furthermore, excess Ca(OH)$_2$ could react with sulphates in ground water, likewise resulting in expansive stresses. Consequently, long-term
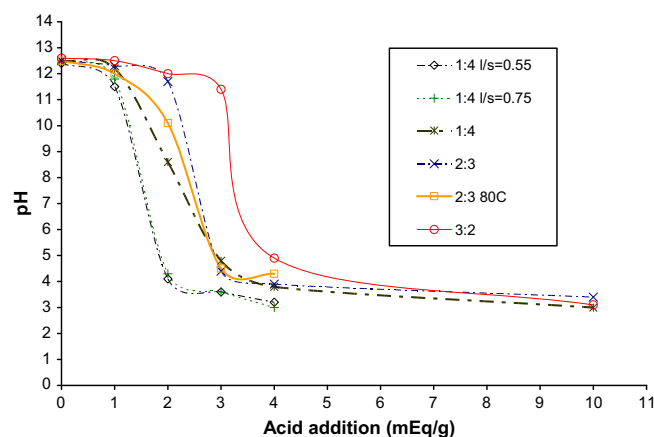

Fig. 9. Acid neutralisation capacity (ANC) of the various mixes according to DD CEN/TS 15364 (2006).

durability testing is required. This is currently underway, but is not the subject of this immediate study.

A consequence of the Ca(OH)$_2$ content was reflected in the acid neutralisation capacity (ANC), as shown in Fig. 9. ANC is an important parameter for S/S products, significantly impacting the leaching behaviour by influencing speciation of contaminants and soundness of monoliths. Stegemann and Cote [80] proposed ANC to pH 9 of 1–3 mEq/g depending on the disposal scenario. The plateau just above pH 12 in the ANC curves is due to buffering by Ca(OH)$_2$ and C–S–H [81,82]. Other metal contaminants influence the ANC, and interactions are often complicated [81,82] but plateaus for other reaction products could not be observed due to the low resolution of the curves obtained. However strong positive correlations between the ANC of this plateau and the Ca(OH)$_2$ content observed by STA suggests the Ca(OH)$_2$ content was pivotal. The l/s ratio had far less effect on the ANC than the APC residue:PFA ratio.

An ANC of untreated APC residues of 6–8 mEq/g to pH 7 has been reported [83], but the ANC of S/S products should be lower than that of the initial residue, since the Ca(OH)$_2$ is consumed in the pozzolanic reactions. Addition of 1–2 mEq/g HNO$_3$ to blends of APC residue/cement and APC residue/GGBS has been reported previously, revealing a plateau in the ANC curve just above pH 12, similar to samples 2:3 and 3:2 in the current study [13,14]. CEM (II) and geopolymeric systems containing municipal solid waste incinerator fly ash, with 1 and 2 mEq/g additions meanwhile showed a lower capacity [44], most likely due to lower Ca(OH)$_2$ contents, but greater pH values than those observed here with additions of 4–6 mEq/g. The different behaviour is due to differences in the reaction products formed.

Along with Ca(OH)$_2$ and CaCO$_3$, Friedel's salt was identified by STA (mass loss at ~175 °C and ~315 °C) [18,85,86]. The presence of these phases, alongside NaCl, quartz, mullite, C–S–H (I), katoite, zeolite Na-P1, sodalite, and vishnevite was confirmed by XRD [86]. However, composition was dependant on mix design and curing conditions and not all phases were present in all of the samples.

3.5. Granular leach

Granular leach tests minimise physical encapsulation thereby offering information on chemical immobilisation. Samples cured for 28 days were tested according to BS EN 12457-2, and the resultant data summarised in Table 5.

The TDS increased with APC residue content, and always exceeded the WAC for SNR of 60,000 mg/kg. Much of the TDS was attributed to soluble chloride species, often NaCl, which also resulted in SNR WAC for chlorides (15,000 mg/kg) being exceeded.

Table 5
Cl$^-$ and SO$_4^{2-}$ leach, pH and TDS during BS EN 12457-2, SO$_4^{2-}$ availability assumes all available sulphur to be present as SO$_4^{2-}$.

Mix	Cl$^-$		SO$_4^{2-}$		pH	TDS (mg/kg)
	Availability (mg/kg)	12457-2 (mg/kg)	Availability (mg/kg)	12457-2 (mg/kg)		
1:4 l/s = 0.55	35,500	26,300	83,100	4900	12.3	175,000
1:4 l/s = 0.75	34,700	27,700	81,300	4350	12.4	149,500
1:4	31,700	21,200	74,400	2850	12.3	120,000
2:3 (23)	65,400	49,500	61,500	4900	12.7	133,500
2:3	62,400	45,900	58,700	2259	12.5	148,500
2:3 (80)	64,700	43,700	60,800	2163	12.5	122,500
3:2	97,800	70,900	45,700	5420	12.5	159,500

Table 6
Cl$^-$ and SO$_4^{2-}$ results for EA NEN 7375 and following tests, ε_{64}^* = measured 64 day release, pD_e = −log diffusion coefficient.

Mix	Chloride				Sulphate				UCS		
	ε_{64}^* (mg/m^2)	pD_e	% release	12457-2 after	ε_{64}^* (mg/m^2)	pD_e	%[b] release	12457-2 after	Before (MPa)	After (MPa)	% loss
1:4 l/s = 0.55	256,500	n/a	67	5480	38,742	n/a	3	2000	13.4	16.8	−25.37
1:4 l/s = 0.75	279,313	n/a	87	380	36,804	n/a	3	0	10.1	8.1	19.80
1:4	234,825	n/a	90	280	22,892	n/a	2.5	0	4.6	2.1	54.35
2:3 (23)	340,646	n/a	63	9690	30,325	11.9	4	2240	3.0	9.6	−220.00
2:3	298,458	10.7	55	13,170	21,167	11.2	2.5	1700	8.7	13.6	−56.32
2:3 (80)	460,833	n/a	85	460	38,663	n/a	5	0	7.9	3.6	54.43
3:2	466,271	11.5	55	22,660	28,938	11.5	4.5	1660	6.5	8.4	−29.23

[b] % results for sulphates were calculated assuming all S to be present as SO$_4^{2-}$ which is believed to be false.

The presence of significant quantities of soluble chlorides is consistent with previous work utilising cements or GGBS [13–15,19]. Despite the majority of chlorides leaching, XRD and thermal analysis of samples following BS EN 12457-2 did reveal retention of some chlorides as Friedel's salt/hydrocalumite and sodalite [86].

Sulphate levels were all considerably below the WAC for SNR (20,000 mg/kg) and XRD suggested their presence as vishnevite. A large proportion of the sulphur was thought to be present in reduced forms rather than sulphates, which would explain the low release. Results for granular leach tests showed, in general, increased sulphate leach corresponding to higher release of chlorides. This is believed to be due to the greater solubility of sulphates in solutions of higher ionic strength [87].

Leachate pH values of around 12.5 suggest Ca(OH)$_2$ was the controlling factor. Higher pHs were seen for samples cured at room temperature suggesting hydrolysis of alkali metal hydroxides, and may be a result of the slower reactions. All samples exceeded the pH boundaries of ~12.2 > pH > ~11.9 suggested by Stegemann and Zhou [45]. This has implications for leachability of amphoteric metals such as Pb and Zn.

Increasing the l/s ratio led to a decrease in TDS, as a result of a greater degree of hydration (and therefore increase in dry mass due to bound water). This increase in dry mass at higher l/s reduced the availability of APC residue (mg/kg$_{dry}$) and therefore the availability of soluble species.

3.6. Monolithic leach

Table 6 shows the chloride and sulphate leach data obtained from monolithic leach tests conducted according to EA NEN 7375. All monoliths remained cohesive throughout the test, and so following monolithic leaching the UCS of each sample was determined as described previously, and the resultant granular material analysed according to BS EN 12457-2 (with data also shown in Table 6), confirming calculations of retained analytes. Samples 2:3(80) and 1:4 samples with l/s = 0.75 or 1 lost strength during monolithic leach testing. These samples also lost the most strength during 7 days submersion (Table 4) and monolithic leach behaviour indicated they were the most permeable samples. Other samples

appeared to gain strength indicating continued hydration and reaction.

Diffusion coefficients calculated from the behaviour during diffusion controlled increments (and presented as the −log pD_e) offer information on the permeability and tortuosity of the matrix. With samples for which there is no diffusion controlled increment diffusion coefficients cannot be calculated. All such samples in this work showed depletion.

Diffusion coefficients and cumulative leach results showed lower percentage release and slower release of chloride from samples with high APC residue contents and lower l/s. Curing at 38 °C gave the greatest extent of encapsulation, supporting earlier comments that high temperature curing can lead to an open microstructure [33,73–75] whilst inferior encapsulation in samples cured at room temperature was likely due to the lesser extent of the pozzolanic reaction, as evidenced from slower strength development.

Rapid chloride release from mixes 1:4 prevented calculations of diffusion coefficients. However the slowed release with reduced l/s could be seen by the reduced percentages released throughout the test and verified by the increased release from the subsequent granular leach tests.

Despite the slower release with higher APC residue content, the cumulative release of chloride from the samples followed expected trends; higher APC residue contents led to greater release due to increased availability (Fig. 10). Differences in measured release from samples with respect to l/s could be explained in terms of variations in dry mass density and compaction upon casting and therefore variable anion availability plus variations in percentage release owing to differences in porosity and permeability.

Surface wash off was observed from mix 3:2; consistent with the observation of a white efflorescence on samples of low consistence. Dissolution of this efflorescence in de-ionised water with subsequent ion chromatography confirmed significant chloride content and XRD analysis revealed it to be NaCl. Such surface wash off leads to under-estimation when calculating derived 64 day release (ε_{64}) from diffusion controlled increments. Thus, the derived cumulative release for mix 3:2 was lower than the measured cumulative release (Table 7). Conversely the depletion which occurred after the 4th fraction of mix 2:3 led to an over-estimation of ε_{64}.

Table 7
Comparison of EA NEN 7375 results for measured cumulative release (ε_{64}^*) and derived cumulative release (ε_{64}) with previous work.

	%w/w APC residue	Available Cl (mg/kg)	ε_{64}^* (mg/m²)	ε_{64} (mg/m²)
CEM I [13]	50	80,000	590,000	1,420,000
CEM I [13]	80	128,000	997,000	3,100,000
CEM I [13]	90	144,000	1,167,000	4,310,000
GGBS [14]	50	n/a	542,000	702,000
PFA (present study)	40 (2:3)	62,400	298,500	746,400
PFA (present study)	60 (3:2)	97,800	466,300	434,300

Comparison of the monolithic leach results from the APC residue:co-fired PFA matrices examined here with matrices using more traditional and expensive CEM I and GGBS binders [13,14] (Table 7) shows greater retention of chlorides in the 2:3 and 3:2 samples than in the other binder systems. The 3:2 sample had a higher APC residue content and chloride availability than samples produced with 50%w/w APC residue and either CEM I or GGBS, yet both measured and derived release over 64 days were lower. Sample 2:3 showed lower measured release but a greater rate of release during the diffusion controlled increment (indicated by ε_{64}) than the GGBS samples. The long setting times of these mixes should be remembered however, samples prepared at higher temperatures showed more practical setting times but little encapsulation.

All samples exceeded the SNR WAC for chloride according to EA NEN 7375 (10,000 mg/kg). Samples also exceeded the SNR WAC for sulphate release (10,000 mg/kg) despite meeting the granular limits, which may suggest release to be highly time dependant.

Cumulative sulphate release was greater from sample 3:2 than sample 1:4 (Fig. 11), despite the lower availability. This is explained by the sustained high release of chlorides from sample 3:2 maintaining a high ionic strength leach environment thus reducing the activity of the sulphate ions and increasing their solubility [87,88]. Consequently, sulphate release was often observed to mimic chloride release for many samples, examples of which are shown in Fig. 12. Sulphate release demonstrated depletion once chloride leach was depletion controlled, regardless of the percentage released. The effect may be considered similar to the greater solubility of Ca(OH)$_2$ reported in NaCl solutions [89]. The ionic strength of the leach environment resulting from the high soluble chloride content clearly has a significant effect on the mobility of many components. This mobility may be particularly prominent when performing regulatory leach tests such as EA NEN 7375 in which the solidified waste is exposed to the solution containing leached ions for prolonged periods of time.

This relationship means that whilst sulphate release appeared to be a problem, the implementation of a washing stage to remove the chloride may bring sulphate release within regulatory limits. The granular leach results obtained from the residue of the monolithic tests showed clearly that samples with negligible chloride contents showed no sulphate release, whilst those still containing chlorides showed continued sulphate release; this occurred irrespective of sulphate availability. A further consequence of this observation is that leachate flowing around the S/S products within landfill sites is highly unlikely to have a low ionic strength, therefore ionic interactions are inevitable and could affect the release of contaminants other than sulphates.

Finally, Fig. 10 also shows the pH of the fractions for each APC residue:PFA ratio and indicates that the pH appeared to stabilise in later fractions. Given that by this point soluble phases will have been removed, the pH at these later stages reflected the principal binding products in the stabilised matrices, such as C–S–H. The pH levels for 1:4, 2:3, and 3:2 of 11.8, 12.0, and 12.3 respectively may suggest that increasing the APC residue:PFA ratio resulted in more calcium-rich hydration products. It is also possible that there is residual Ca(OH)$_2$ in 3:2 which is controlling the pH. Chen et al. [90] leached synthetic C–S–H samples and showed a reduction in pH upon removal of calcium, with a pH of 11.8 for a Ca/Si ratio of 1.21. Samples prepared at 1:4, with a pH of 11.8, showed the lowest strengths, highest porosities and evidence of open, porous microstructures. Whilst the precise composition of the binding phases was not determined, it may be assumed that some stable hydration products were present due to the retention of a cohesive matrix with UCS >1 MPa even after 64 days submersion.
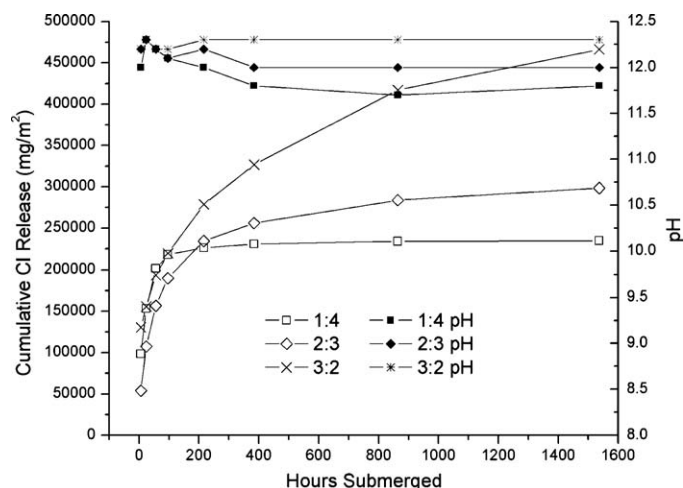

Fig. 10. pH and cumulative Cl release during EA NEN 7375 (mg/m²) from 28 day samples at l/s = 1, cured at 38 °C with varying APC residue:PFA.
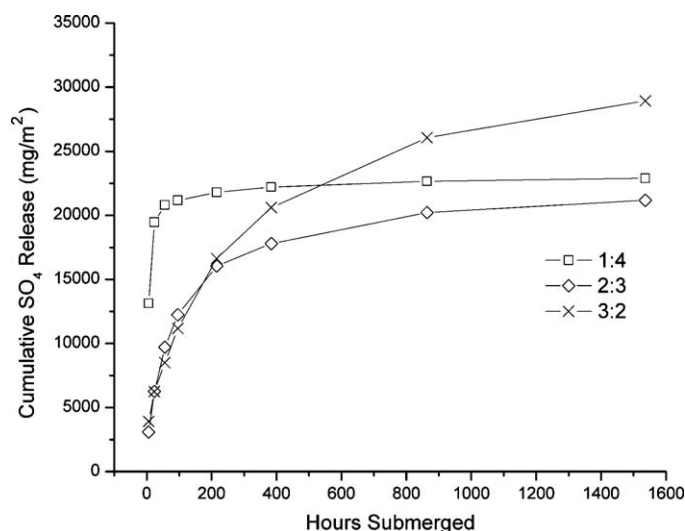

Fig. 11. Cumulative SO$_4$ release during EA NEN 7375 (mg/m²) from 28 day samples at l/s = 1, cured at 38 °C with varying APC residue:PFA.
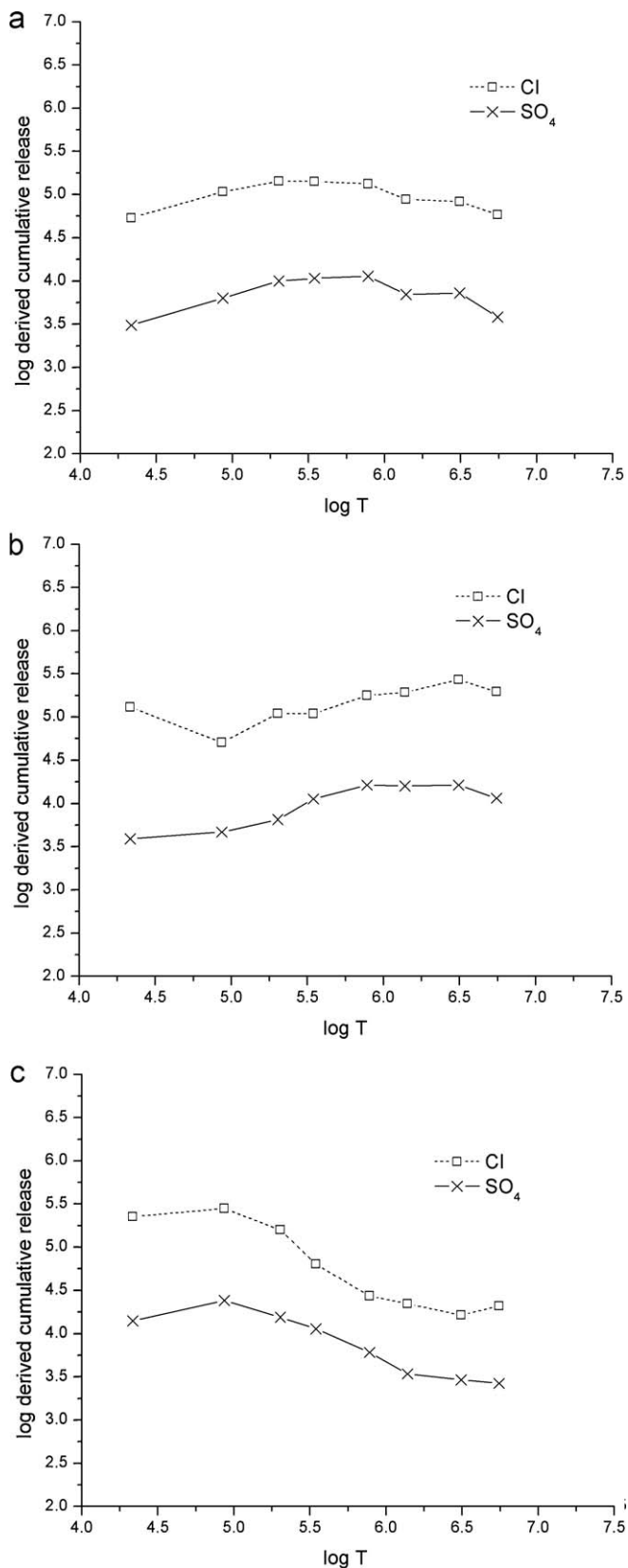
Fig. 12. Log–log plots of Cl and SO_4 release according to EA NEN 7375 (a) 2:3, (b) 3:2, and (c) 2:3 (80).

4. Conclusions

Waste alkali activation of APC residue/co-fired PFA blends produced monoliths of significant unconfined compressive strength (UCS) by pozzolanic reactions. The matrices maintained soundness during 64 days exposure to water according to EA NEN 7375.

Under ambient conditions solidification occurred very slowly resulting in unfeasibly long setting times and strength development for commercial application. Increasing the curing temperature led to a dramatic reduction in setting time and increased the rate of strength development but excessive temperatures reduced long term strength and reduced the physical encapsulation offered by the resultant S/S product.

The use of co-fired PFA, with high sulphur content, caused problems when trying to meet the WAC. Sulphate release was problematic during regulatory monolithic leaching (EA NEN 7375). This was likely due to the high ionic strength of the leachate solution, resulting from the soluble salt wash out. Solute–solvent ion effects increased the solubility of sulphates.

Chloride immobilisation in the systems was shown by granular and monolithic leach tests to be predominantly dependent on physical encapsulation and well above SNR WAC without a washing stage being implemented. This was explained by identification of the majority of the chloride as halite. The extent of physical encapsulation was seen for some samples to be greater than that observed using more expensive cement and GGBS binders. Slowed release by encapsulation would be dependent on the monoliths maintaining their structural integrity. The long term soundness of the blends used in this study has not been examined, but deserves further investigation.

References

[1] EC, European Waste Catalogue, Commission Decision 2000/532/EC, 2002.
[2] The Landfill (England and Wales) (Amendment) Regulations, 2005.
[3] EA, Solid Residues from Municipal Waste Incinerators in England and Wales, A Report on an Investigation by the Environment Agency, 2002.
[4] T. Astrup, K. Crillesen, K. Bojsen, H. Ornebjerg, R. Morin, J.-F. Brua, H. Friege, C. Bader, Management of APC Residues from W-t-E Plants an Overview of Management Options and Treatment Methods, ISWA-WG Thermal Treatment of Waste, 2008.
[5] Defra, Waste Strategy for England, 2007.
[6] EC, EU landfill directive, council directive 1999/31/EC of 26 April 1999 on the landfill of waste, Official Journal L182 (1999) 0001–0019.
[7] A. Metcalfe, Incineration transformation, in: CIWM, The Journal for Waste and Resource Management Professionals, June 2010.
[8] Defra/EA, Landfill Regulations – Defra/Environment Agency Approach to the Use of Higher Waste Acceptance Criteria (WAC) Limits, 2006.
[9] T. Van Gerven, D. Geysen, L. Stoffels, M. Jaspers, G. Wauters, C. Vandecasteele, Management of incinerator residues in Flanders (Belgium) and in neighbouring countries. A comparison, Waste Management 25 (2005) 75–87.
[10] D. Amutha Rani, A.R. Boccaccini, D. Deegan, C.R. Cheeseman, Air pollution control residues from waste incineration: current UK situation and assessment of alternative technologies, Waste Management 28 (2008) 2279–2292.
[11] M.J. Quina, J.C. Bordado, R.M. Quinta-Ferreira, Treatment and use of air pollution control residues from MSW incineration: an overview, Waste Management 28 (2008) 2097–2121.
[12] H.S. Shi, L.L. Kan, Leaching behavior of heavy metals from municipal solid wastes incineration (MSWI) fly ash used in concrete, Journal of Hazardous Materials 164 (2009) 750–754.
[13] C. Lampris, J.A. Stegemann, C.R. Cheeseman, Solidification/stabilisation of air pollution control residues using Portland cement: physical properties and chloride leaching, Waste Management 29 (2009) 1067–1075.
[14] C. Lampris, J.A. Stegemann, C.R. Cheeseman, Chloride leaching from air pollution control residues solidified using ground granulated blast furnace slag, Chemosphere 73 (2008) 1544–1549.
[15] S. Auer, H.J. Kuzel, H. Pollmann, F. Sorrentino, Investigation on MSW fly-ash treatment by reactive calcium aluminates and phases formed, Cement and Concrete Research 25 (1995) 1347–1359.
[16] V. Albino, R. Cioffi, L. Santoro, G.L. Valenti, Stabilization of residue containing heavy metals by means of matrices generating calcium trisulphoaluminate and silicate hydrates, Waste Management & Research 14 (1996) 29–41.
[17] N. Alba, E. Vazquez, S. Gasso, J.M. Baldasano, Stabilization/solidification of MSW incineration residues from facilities with different air pollution control systems. Durability of matrices versus carbonation, Waste Management 21 (2001) 313–323.

[18] P. Ubbriaco, D. Calabrese, Solidification and stabilization of cement paste containing fly ash from municipal solid waste, Thermochimica Acta 321 (1998) 143–150.
[19] C. Lampris, J.A. Stegemann, M. Pellizon-Birelli, G.D. Fowler, C.R. Cheeseman, Metal leaching from monolithic stabilised/solidified air pollution control residues, Journal of Hazardous Materials 185 (2011) 1115–1123.
[20] B.D. Bone, L.H. Barnard, D.I. Boardman, P.J. Carey, C.D. Hills, H.M. Jones, C.L. MacLeod, M. Tyrer, Review of Scientific Literature on the Use of Stabilisation/Solidification for the Treatment of Contaminated Soil, Solid Waste and Sludges, Environment Agency, 2004.
[21] Q.Y. Chen, M. Tyrer, C.D. Hills, X.M. Yang, P. Carey, Immobilisation of heavy metal in cement-based solidification/stabilisation: a review, Waste Management 29 (2009) 390–403.
[22] G. Cornelis, C.A. Johnson, T. Van Gerven, C. Vandecasteele, Leaching mechanisms of oxyanionic metalloid and metal species in alkaline solid wastes: a review, Applied Geochemistry 23 (2008) 955–976.
[23] M.L.D. Gougar, B.E. Scheetz, D.M. Roy, Ettringite and C–S–H Portland cement phases for waste ion immobilization: a review, Waste Management 16 (1996) 295–303.
[24] H.A.F. Dehwah, Effect of sulphate contamination on chloride-binding capacity of plain and blended cements, Advances in Cement Research 18 (2006) 7–15.
[25] EN, 450 Fly Ash for Concrete – Part 1: Definition, Specifications and Conformity Criteria, 2005.
[26] C.S. Poon, X.C. Qiao, Z.S. Lin, Pozzolanic properties of reject fly ash in blended cement pastes, Cement and Concrete Research 33 (2003) 1857–1865.
[27] C.S. Poon, X.C. Qiao, Z.S. Lin, Effects of flue gas desulphurization sludge on the pozzolanic reaction of reject-fly-ash-blended cement pastes, Cement and Concrete Research 34 (2004) 1907–1918.
[28] C.S. Poon, X.C. Qiao, C.R. Cheeseman, Applications of rejected fly ash in stabilisation and solidification processes, in: A.-T. A, J.A. Stegemann (Eds.), Stabilisation/Solidification Treatment and Remediation, A.A. Balkema Publishers, University of Cambridge, 2005.
[29] D. Roy, Alkali-activated cements – opportunities and challenges, Cement and Concrete Research 29 (1999) 249–254.
[30] C.J. Shi, A. Fernandez-Jimenez, Stabilization/solidification of hazardous and radioactive wastes with alkali-activated cements, Journal of Hazardous Materials 137 (2006) 1656–1663.
[31] D.M. Roy, W.M. Jiang, M.R. Silsbee, Chloride diffusion in ordinary, blended, and alkali-activated cement pastes and its relation to other properties, Cement and Concrete Research 30 (2000) 1879–1884.
[32] F. Puertas, S. Martinez-Ramirez, S. Alonso, T. Vazquez, Alkali-activated fly ash/slag cement – strength behaviour and hydration products, Cement and Concrete Research 30 (2000) 1625–1632.
[33] K. Wang, S.P. Shah, A. Mishulovich, Effects of curing temperature and NaOH addition on hydration and strength development of clinker-free CKD-fly ash binders, Cement and Concrete Research 34 (2004) 299–309.
[34] S.D. Wang, K.L. Scrivener, Hydration products of alkali-activated slag cement, Cement and Concrete Research 25 (1995) 561–571.
[35] P. Lu, Q. Li, J.P. Zhai, Mineralogical characterizations and reaction path modeling of the pozzolanic reaction of fly ash-lime systems, Journal of the American Ceramic Society 91 (2008) 955–964.
[36] X. Querol, N. Moreno, J.C. Umana, A. Alastuey, E. Hernandez, A. Lopez-Soler, F. Plana, Synthesis of zeolites from coal fly ash: an overview, International Journal of Coal Geology 50 (2002) 413–423.
[37] J.L. Larosa, S. Kwan, M.W. Grutzeck, Zeolite formation in class F fly-ash blended cement pastes, Journal of the American Ceramic Society 75 (1992) 1574–1580.
[38] J.S. Qian, C.J. Shi, Z. Wang, Activation of blended cements containing fly ash, Cement and Concrete Research 31 (2001) 1121–1127.
[39] C.J. Shi, R.L. Day, Acceleration of the reactivity of fly-ash by chemical activation, Cement and Concrete Research 25 (1995) 15–21.
[40] C.J. Shi, Strength, pore structure and permeability of alkali-activated slag mortars, Cement and Concrete Research 26 (1996) 1789–1799.
[41] I. Kourti, D. Amutha Rani, D. Deegan, A.R. Boccaccini, C.R. Cheeseman, Production of geopolymers using glass produced from DC plasma treatment of air pollution control (APC) residues, Journal of Hazardous Materials 176 (2010) 704–709.
[42] I. Lancellotti, E. Kamseu, M. Michelazzi, L. Barbieri, A. Corradi, C. Leonelli, Chemical stability of geopolymers containing municipal solid waste incinerator fly ash, Waste Management 30 (2010) 673–679.
[43] Lei Zheng, Chengwen Wang, Wei Wang, Yunchun Shi, X. Gao, Immobilization of MSWI fly ash through geopolymerization: effects of water-wash, Waste Management 31 (2011) 311–317.
[44] Y. Luna Galiano, C. Fernández Pereira, J. Vale, Stabilization/solidification of a municipal solid waste incineration residue using fly ash-based geopolymers, Journal of Hazardous Materials 185 (2010) 373–381.
[45] J.A. Stegemann, Q. Zhou, Screening tests for assessing treatability of inorganic industrial wastes by stabilisation/solidification with cement, Journal of Hazardous Materials 161 (2009) 300–306.
[46] N. Alba, S. Gasso, T. Lacorte, J.M. Baldasano, Characterization of municipal solid waste incineration residues from facilities with different air pollution control systems, Journal of the Air & Waste Management Association 47 (1997) 1170–1179.
[47] K.Y. Chiang, C.C. Tsai, K.S. Wang, Comparison of leaching characteristics of heavy metals in APC residue from an MSW incinerator using various extraction methods, Waste Management 29 (2009) 277–284.
[48] P.J. He, H. Zhang, C.G. Zhang, D.J. Lee, Characteristics of air pollution control residues of MSW incineration plant in Shanghai, Journal of Hazardous Materials 116 (2004) 229–237.
[49] M.J. Quina, R.C. Santos, J.C. Bordado, R.M. Quinta-Ferreira, Characterization of air pollution control residues produced in a municipal solid waste incinerator in Portugal, Journal of Hazardous Materials 152 (2008) 853–869.
[50] P. Tansens, A.T. Rodal, C.M.M. Machado, H.M.V.M. Soares, Recycling of aluminum and caustic soda solution from waste effluents generated during the cleaning of the extruder matrixes of the aluminum industry, Journal of Hazardous Materials 187 (2011) 459–465.
[51] EN, 13395-1 Products and Systems for the Protection and Repair of Concrete Structures. Test Methods. Determination of Workability. Test for Flow of Thixotropic Mortars, 2002.
[52] EN, 480-2 Admixtures for Concrete, Mortar and Grout. Test Methods. Determination of Setting Time, 2006.
[53] EN, 12390-3, Testing Hardened Concrete. Compressive Strength of Test Specimens, 2009.
[54] EN, 12457-2, Characterisation of Waste. Leaching. Compliance Test for Leaching of Granular Waste Materials and Sludges. One Stage Batch Test at a Liquid to Solid Ratio of 10 l/kg for Materials with Particle Size Below 4 mm (Without or With Size Reduction), 2002.
[55] EA, NEN, Leaching Characteristics of Moulded or Monolithic Building and Waste Materials Determination of Inorganic Components with the Diffusion Test 'The Tank Test', 2004.
[56] CEN/TS, 15364, Characterization of Waste. Leaching Behaviour Tests. Acid and Base Neutralization Capacity Test, 2006.
[57] Z. Abbas, A.P. Moghaddam, B.M. Steenari, Release of salts from municipal solid waste combustion residues, Waste Management 23 (2003) 291–305.
[58] D. Geysen, C. Vandecasteele, M. Jaspers, E. Brouwers, G. Wauters, Effect of improving flue gas cleaning on characteristics and immobilisation of APC residues from MSW incineration, Journal of Hazardous Materials 128 (2006) 27–38.
[59] D. Geysen, C. Vandecasteele, M. Jaspers, G. Wauters, Comparison of immobilisation of air pollution control residues with cement and with silica, Journal of Hazardous Materials 107 (2004) 131–143.
[60] F. Bodenan, P. Deniard, Characterization of flue gas cleaning residues from European solid waste incinerators: assessment of various Ca-based sorbent processes, Chemosphere 51 (2003) 335–347.
[61] W. Jozewicz, B.K. Gullett, Reaction mechanisms of dry Ca-based sorbents with gaseous HCl, Industrial & Engineering Chemistry Research 34 (1995) 607–612.
[62] S. Diamond, On the glass present in low-calcium and high-calcium fly ashes, Cement and Concrete Research 13 (1983) 459–464.
[63] F.P. Glasser, Fundamental aspects of cement solidification and stabilisation, Journal of Hazardous Materials 52 (1997) 151–170.
[64] B. Liang-Man, L. Jun, L. Wei, L. Wen-Zhong, Z. Gui-Lin, L. Yan, M. Chen-Yan, Z. Yi-Dong, H. Wei, H. Tian-Dou, Investigation of sulfur speciation in particles from small coal-burning boiler by XANES spectroscopy, Chinese Physics C 33 (2009) 1001–1005.
[65] R.K. Dhir, F.H. Hubbard, J.G.L. Munday, M.R. Jones, S.L. Duerden, Contribution of PFA to concrete workability and strength development, Cement and Concrete Research 18 (1988) 277–289.
[66] J. Paya, J. Monzo, M.V. Borrachero, E. Perris, F. Amahjour, Thermogravimetric methods for determining carbon content in fly ashes, Cement and Concrete Research 28 (1998) 675–686.
[67] S. Asavapisit, G. Fowler, C.R. Cheeseman, Solution chemistry during cement hydration in the presence of metal hydroxide wastes, Cement and Concrete Research 27 (1997) 1249–1260.
[68] I.F. Olmo, E. Chacon, A. Irabien, Influence of lead, zinc, iron (III) and chromium (III) oxides on the setting time and strength development of Portland cement, Cement and Concrete Research 31 (2001) 1213–1219.
[69] K.L. Lin, K.S. Wang, C.Y. Lin, C.H. Lin, The hydration properties of pastes containing municipal solid waste incinerator fly ash slag, Journal of Hazardous Materials 109 (2004) 173–181.
[70] H.F.W. Taylor, Cement Chemistry, Thomas Telford, 1997.
[71] A.M. Neville, Properties of Concrete, 4th ed, Longman Scientific & Technical, Harlow, 1995.
[72] S. Hanehara, F. Tomosawa, M. Kobayakawa, K. Hwang, Effects of water/powder ratio, mixing ratio of fly ash, and curing temperature on pozzolanic reaction of fly ash in cement paste, Cement and Concrete Research 31 (2001) 31–39.
[73] K.O. Kjellsen, R.J. Detwiler, Reaction kinetics of Portland cement mortars hydrated at different temperatures, Cement and Concrete Research 22 (1992) 112–120.
[74] K.O. Kjellsen, R.J. Detwiler, O.E. Gjorv, Pore structure of plain cement pastes hydrated at different temperatures, Cement and Concrete Research 20 (1990) 927–933.
[75] J. Skalny, I. Odler, Pore structure of hydrated calcium silicates. 3. Influence of temperature on pore structure of hydrated tricalcium silicate, J. Colloid Interface Sci. 40 (1972) 199–205.
[76] A. Antemir, C.D. Hills, P.J. Carey, K.H. Gardner, E.R. Bates, A.K. Crumbie, Long-term performance of aged waste forms treated by stabilization/solidification, Journal of Hazardous Materials 181 (2010) 65–73.
[77] D. Bonen, S.L. Sarkar, The effects of simulated environmental attack on immobilisation of heavy-metals doped in cement based materials, Journal of Hazardous Materials 40 (1995) 321–335.

[78] F. Sanchez, C. Gervais, A.C. Garrabrants, R. Barna, D.S. Kosson, Leaching of inorganic contaminants from cement-based waste materials as a result of carbonation during intermittent wetting, Waste Management 22 (2002) 249–260.

[79] P. Purnell, E. Farahi, N.R. Short, Supercritical carbonation of lime based sustainable structural ceramics, Advances in Applied Ceramics 109 (2010) 280–286.

[80] J.A. Stegemann, P.L. Cote, A proposed protocol for evaluation of solidified wastes, Science of the Total Environment 178 (1996) 103–110.

[81] C. Shi, J.A. Stegemann, Acid corrosion resistance of different cementing materials, Cement and Concrete Research 30 (2000) 803–808.

[82] J.A. Stegemann, A.S.R. Perera, C. Cheeseman, N.R. Buenfeld, 1/8 factorial study of metal effects on acid neutralization by cement, Journal of Environmental Engineering-ASCE 126 (2000) 925–933.

[83] M.J. Quina, J.C.M. Bordado, R.M. Quinta-Ferreira, The influence of pH on the leaching behaviour of inorganic components from municipal solid waste APC residues, Waste Management 29 (2009) 2483–2493.

[85] U.A. Birnin-Yauri, F.P. Glasser, Friedel's salt, $Ca_2Al(OH)_6(Cl,OH).2H_2O$: its solid solutions and their role in chloride binding, Cement and Concrete Research 28 (1998) 1713–1723.

[86] R. Shirley, L. Black, Alkali activated solidification/stabilisation of APC residue using co-fired PFA: mineralogical characterisation, Adv. Appl. Ceram., in press.

[87] J.D. Willey, The effect of ionic strength on the solubility of an electrolyte, J. Chem. Educ. 81 (2004) 1644–1646.

[88] M.E. Essington, Soil and water chemistry: an integrative approach, 2004.

[89] F.P. Glasser, J. Pedersen, K. Goldthorpe, M. Atkins, Solubility reactions of cement components with NaCl solutions: I. $Ca(OH)_2$ and C–S–H, Advances in Cement Research 17 (2005) 57–64.

[90] J.J. Chen, J.J. Thomas, H.F.W. Taylor, H.M. Jennings, Solubility and structure of calcium silicate hydrate, Cement and Concrete Research 34 (2004) 1499–1519.